Int. J. Electrochem. Sci., 6 **(2011)** 2912 - 2931

International Journal of
ELECTROCHEMICAL
SCIENCE
www.electrochemsci.org

Adsorption and Corrosion Inhibition Properties of Cefadroxil on Mild Steel in Hydrochloric Acid

Sudhish K. Shukla[1,*], *M. A. Quraishi*[2] *and Eno E. Ebenso*[1]

[1] Department of Chemistry, School of Mathematical and Physical Sciences,
North West University(Mafikeng Campus), Private Bag X2046, Mmabatho 2735, South Africa
[2] Department of Applied Chemistry,Institute of Technology, Banaras Hindu University,
Varanasi 221005, India
[*]E-mail: sudhish.shukla@gmail.com

Received: 21 May 2011 / *Accepted:* 15 June 2011 / *Published:* 1 July 2011

Corrosion inhibition of mild steel in 1M HCl by cefadroxil has been studied using electrochemical impedance spectroscopy (EIS), potentiodynamic polarization and weight loss methods. The inhibitor showed more than 96% inhibition efficiency at optimum concentration of 11.0×10^{-4} mol l^{-1}. The results obtained by these techniques were well supported by the atomic force microscopy. Thermodynamic parameters obtained support physical adsorption mechanism and the experimental data fits well into the Langmuir adsorption isotherm model. Potentiodynamic polarization suggests that cefadroxil act as mixed type inhibitor. Thermodynamic parameters suggest the adsorption is spontaneous and exothermic process. The results obtained from the three methods used are in good agreement.

Keywords: Cefadroxil, Mild steel, AFM, Weight loss, EIS, Adsorption

1. INTRODUCTION

Corrosion of mild steel is most common type of corrosion in acidic solution. It has practical importance in acid pickling, chemical scale cleaning, in metallurgy, in petrochemical industry etc. Hydrochloric acid is most common type of acid used in the various industries. This leads to the researchers to study the effect of corrosion inhibitors on mild steel in hydrochloric acid solutions. [1-5]. Most common type of corrosion inhibitors are organic compounds. Their inhibition property is dependent upon their functional group, which adsorb on the metal surface. Most of the efficient organic compounds acts as inhibitors have oxygen, sulphur, nitrogen atoms and multiple bonds through which they adsorb on metal surface [6-8]. A large number of organic compounds have been used as corrosion inhibitors for mild steel and most of them are highly toxic to both human beings and

environment both. Due to the increasing environmental awareness and the negative effects of some chemicals, research activities in recent times are geared towards developing the less toxic and environmentally safe corrosion inhibitors [9-14]

The present article is devoted to the study of Cefadroxil as corrosion inhibitor for mild steel in hydrochloric acid solution using electrochemical impedance spectroscopy (EIS), potentiodynamic polarization, weight-loss and atomic force microscopy (AFM) techniques.

Cefadroxil is the commercial name for (6R, 7R)-7-{[(2R)-2-amino-2-(4-hydroxyphenyl) acetyl] amino}-3-methyl-8-oxo-5-thia-1-azabicyclo[4.2.0]oct-2-ene-2-carboxylic acid having molecular formula $C_{16}H_{17}N_3O_5S$. Molecular mass of the Cefadroxil is 363.389 g/mol. It is a broad spectrum antibiotic that is active against both Gram-positive and Gram -negative bacteria. It is used for the treatment of pneumonia, acute bronchitis, urinary tract infection, skin and soft tissue infections, septicemia and anthrax. Its chemical structure is shown in Figure 1.

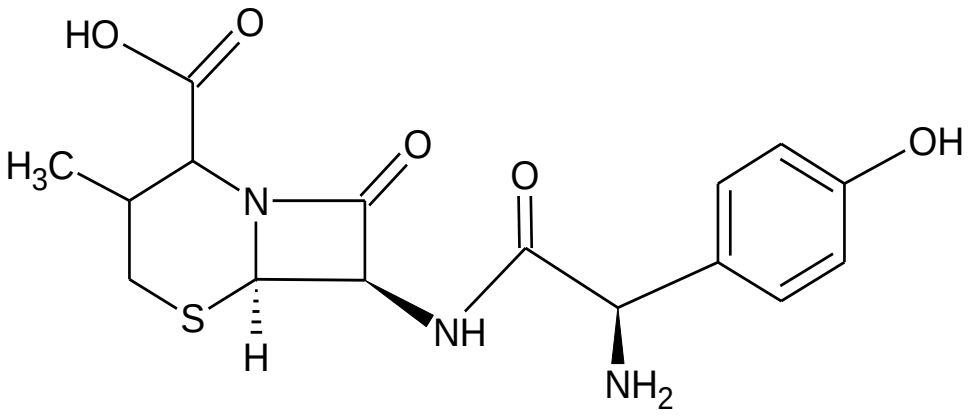

Figure 1. Structure of cefadroxil molecule

2. EXPERIMENTAL

2.1. Inhibitor

Stock solution of Cefadroxil was made in 10:1 ratio of water: ethanol mixture by volume to ensure the solubility. All the experiments were carried out using this stock solution.

2.2. Corrosion measurements

Prior to all measurements, the mild steel specimens having composition (wt %): C 0.14, Mn 0.035, Si 0.17, S 0.025, P 0.03 and balance Fe were abraded successively with emery papers from 600 to 1200 mesh in^{-1}grade. The specimen were washed with double distilled water, degreased with acetone and dried in hot air blower. After drying, the specimen were placed in desiccators and then used for the various experiments. The aggressive solution of 1M HCl was prepared by the dilution of

analytical grade hydrochloric acid (37%) with double distilled water and all the experiments were carried out in the unstirred solutions.

The weight loss study was carried out on mild steel strips of 5.0cm x 2.0cm x 0.025cm dimension. The electrochemical measurements were carried out on mild steel strips with the dimension 1.0cm x 1.0cm exposed with a 7.5 cm long stem (coated by the commercially available lacquer).

2.3. Electrochemical impedance spectroscopy

The EIS tests were performed at 308±1K in a three electrode assembly. A saturated calomel electrode was used as a reference and a 1 cm^2 platinum foil was used as counter electrode. All the potentials were measured versus SCE. The electrochemical impedance spectroscopy measurements were perform using a Gamry instrument potentiostat / galvanostat with a Gamry framework system based on ESA 400 in a frequency range 10^{-2}Hz – 10^5 Hz under potentiodynamic conditions with amplitude of 10 mV peak to peak, using AC signal at E_{corr}. Gamry applications include software DC105 for corrosion and EIS300 for EIS measurements and Echem analyst version 5.50 software packages for data fitting. The experiments were carried out after 30 minutes of immersion in the test solution without deaeration and stirring.

The inhibition efficiency of the inhibitor was calculated from the charge transfer resistance values using following equation:

$$\mu_{R_t} = \frac{(1/R_t^o) - (1/R_t^i)}{(1/R_t^o)} \times 100 \quad (1)$$

where R_t^o and R_t^i are the charge transfer resistances in the absence and in presence of inhibitor respectively.

2.4. Potentiodynamic polarization

The electrochemical behavior of mild steel sample in inhibited and non-inhibited solution was studied by recording anodic and cathodic potentiodynamic polarization curves. Measurements were performed in the 1M HCl solution containing different concentrations of the tested inhibitor by changing the electrode potential automatically from −250 to +250mV versus corrosion potential at a scan rate of $1mVs^{-1}$. The linear Tafel segments of anodic and cathodic curves were extrapolated to corrosion potential to obtain corrosion current densities (I_{corr}).

The inhibition efficiency was evaluated from the measured I_{corr} values using the following relationship:

$$\eta_p = \frac{I_{corr}^o - I_{corr}^i}{I_{corr}^o} \times 100 \quad (2)$$

where I^{o}_{corr} and I^{i}_{corr} are the corrosion current densities in the absence and presence of inhibitor, respectively.

2.5. Linear polarization measurement

The linear polarization study were carried out from cathodic potential of -0.02V vs OCP to an anodic potential of +0.02V vs OCP at a sweep rate 0.125 mVs^{-1} to study the polarization resistance ($R_{p)}$ in 1 M HCl solution with and without different concentration of inhibitor. Polarization resistance (R_p) was evaluated from the slope of the curve in the vicinity of the corrosion potential. The inhibition efficiency was calculated from the polarization resistance values by the relationship as follows:

$$\mu_{R_p} = \frac{(1/R_p^o) - (1/R_p^i)}{(1/R_p^o)} \times 100 \quad (3)$$

where R_p^o and R_p^i are the polarization resistance in absence and presence of inhibitor, respectively.

2.6. Weight loss measurements:

Weight loss or gravimetric measurements were performed on mild steel sample by immersing it in the absence and presence of different concentrations of cefadroxil at 35°C for 3h duration in 1M HCl solution. The inhibition efficiency (%) was determined using the following equation:

$$\eta_{WL} = \frac{W_o - W_i}{W_o} \times 100 \quad (4)$$

where W_o and W_i are the weight loss values in absence and presence of inhibitor. The weight loss measurements were also carried out at different time intervals, different concentrations of the acid solution and at different temperatures.

2.7. Surface Characterization

The surface morphology of the mild steel specimen was investigated by using atomic force microscopic technique. The atomic force microscopy was performed using NT-MDT multimode AFM Russia, controlled by Solver scanning probe microscope controller.

3. RESULTS AND DISCUSSIONS

3.1. Electrochemical impedance spectroscopy

Electrochemical impedance spectroscopy measurements were carried out inorder to study the kinetics of the electrode process and the surface properties of the studied system. This method is

widely used to investigate the corrosion inhibition process [15]. Nyquist and Bode plots of mild steel in 1M HCl solution in absence and presence of different concentrations of cefadroxil are shown in Figure 2a and 2b-c respectively.

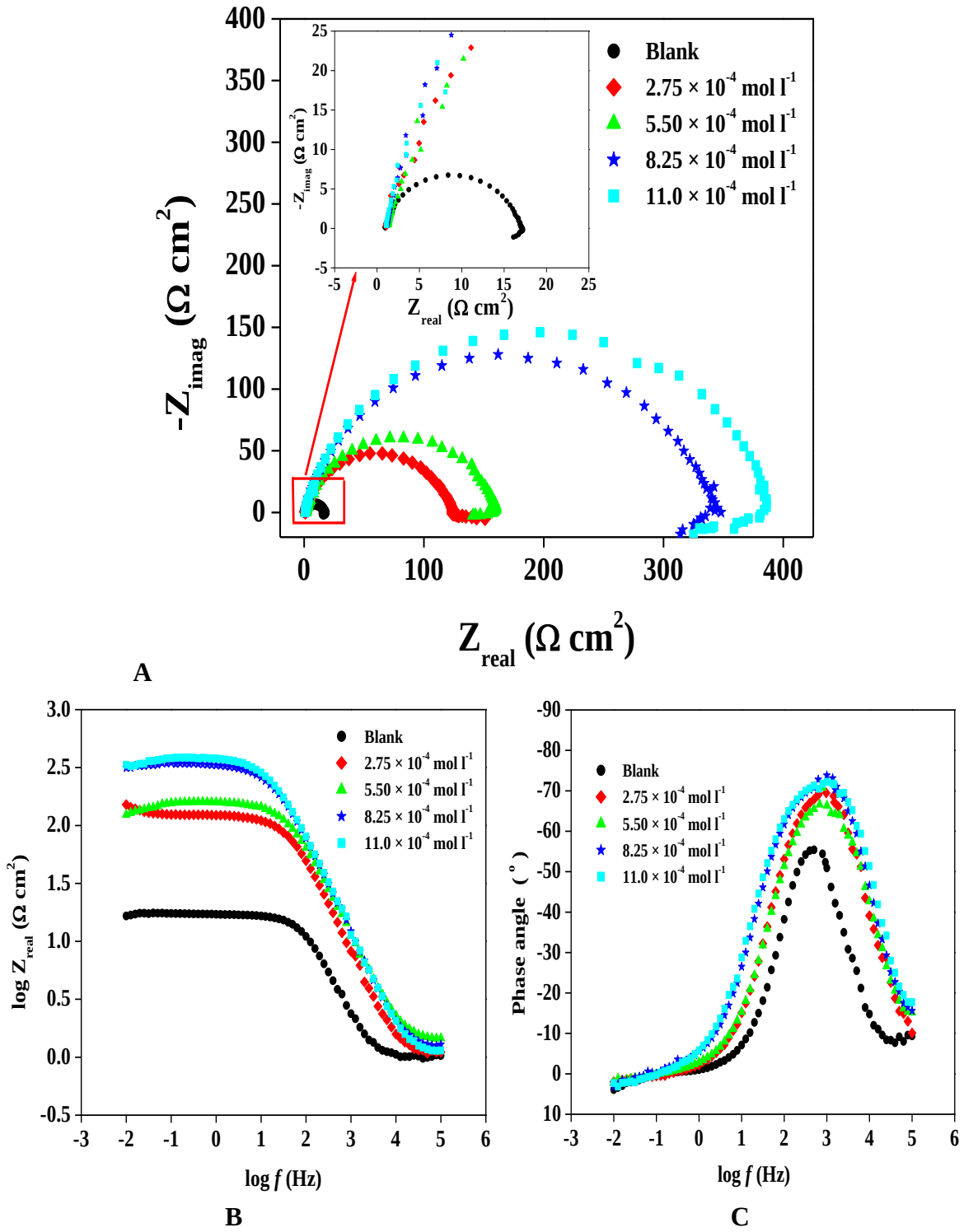

Figure 2. Electrochemical impedance plots (A) Nyquist plot (B) Bode magnitude plot (C) phase angle plot; for the mild steel in absence and presence of different concentrations of cefadroxil

In Nyquist plot shown in Figure 2a, a high frequency depressed charge transfer semicircle is observed. Figure 2b suggests a onetime constant Bode plot. The high frequency semicircle is attributed to the time constant of charge transfer and double layer capacitance [16, 17]. The charge transfer resistance increment raises the tendency of current to pass through the capacitor of the circuit. It is clear from the figure 2a that the impedance spectra is not a perfect semicircle and the depressed capacitive loop corresponds to surface heterogeneity which may be the result of surface roughness, dislocation, distribution of active sites, or adsorption of the inhibitor molecules[18 - 20]. The phase angle at higher frequencies is attributed anticorrosion performance. The more negative the phase angle, the more capacitive the electrochemical behavior [21]. The depression of phase angle at relaxation frequency with the decrease in the cefadroxil concentration indicates decrease of capacitive response with the decrease of inhibitor concentration. Such a phenomenon indicates higher corrosion activity at low concentrations of the inhibitor [22].

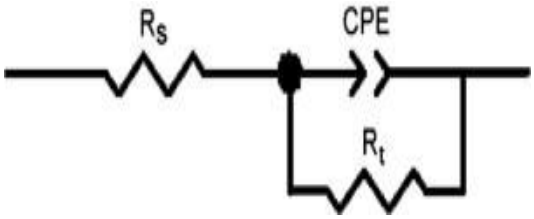

Figure 3. The electrochemical equivalent circuit used to fit the impedance measurements.

The measured data were analyzed using the equivalent circuit given in figure 3. This circuit generally used to describe the iron/acid interface model [23]. This circuit gives an accurate fit to all experimental impedance data for cefadroxil. The experimental data simulated with the equivalent circuit to Bode plot in the presence of 11.0×10^{-4} mol l^{-1} inhibitor are presented in Figure 4(a-b). The equivalent circuit consists of solution resistance (R_s), charge transfer resistance (R_t) and a constant phase angle (CPE).

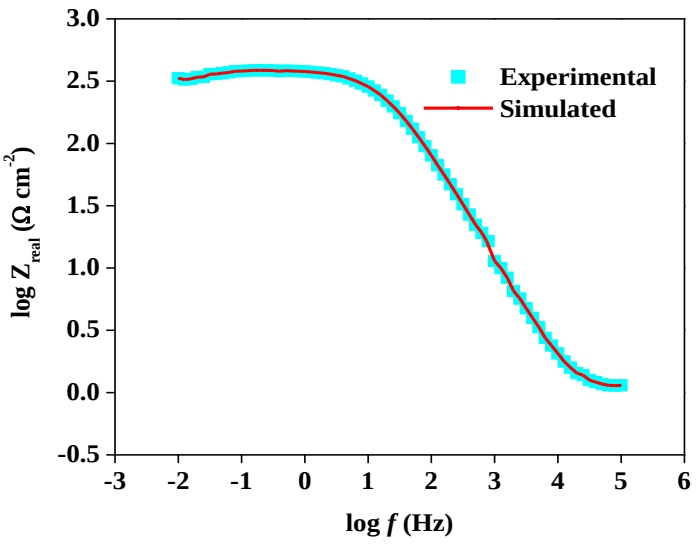

A

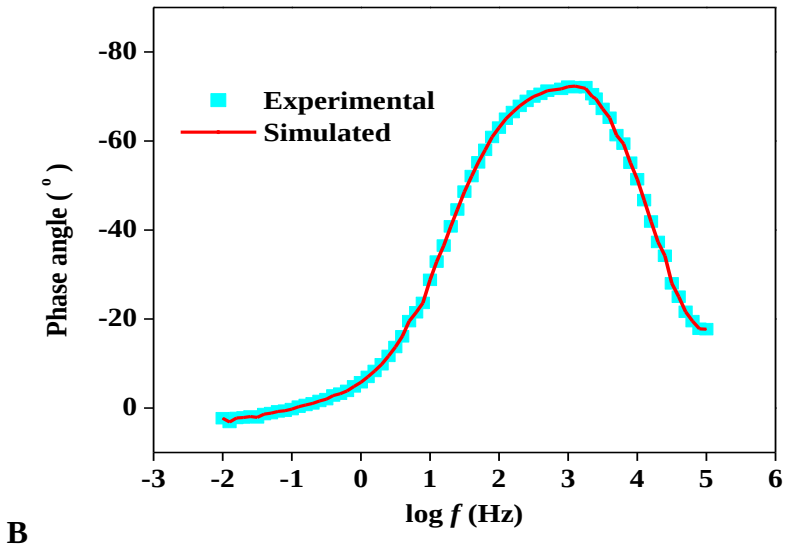

B

Figure 4. Experimental and simulated fit of impedance measurement (A) bode magnitude plot (B) phase angle plot; of mild steel in 1M HCl in presence of 11.0×10^{-4} mol l^{-1}.

The impedance function of CPE is as follows:

$$Z_{CPE} = Y^{-1}(j\omega)^{-n} \quad (5)$$

where, Y is the magnitude of the CPE, ω is the angular frequency and the deviation parameter n is a valuable criterion of the nature of the metal surface and reflects microscopic fluctuations of the surface. For n=0, Z_{CPE} represents a resistance with $R=Y^{-1}$; n=-1 and inductance with $L=Y^{-1}$ and n=1 an ideal capacitor with $C=Y$ [24]. In iron/steel system ideal capacitor behavior is not observed due to the roughness and /or uneven current distributions on the electrode surface resulting in the frequency depression [25, 26]. The electrochemical parameters R_s, R_t, Y_o and n, obtained from the fitting of the recorded data using the equivalent circuit and listed in Table 1.

Table 1. Electrochemical impedance spectroscopy parameters for mild steel in 1M HCl in absence and presence of different concentrations of cefadroxil.

Inhibitor conc. (10^{-4} × mol l^{-1})	**R_s (Ω cm^2)**	**R_t (Ω cm^2)**	**n**	**Y_o (10^{-6} Ω^{-1} cm^{-2})**	**C_{dl} (μF cm^{-2})**	**μ_{R_t} (%)**
Blank	0.975	17.2	0.881	224	104	-
2.75	0.990	124.6	0.858	68	39	86.2
5.50	1.302	159.9	0.842	60	31	89.2
8.25	1.102	347.8	0.848	51	25	95.1
11.0	0.967	368.8	0.854	48	24	95.3

C_{dl} values listed in Table 1 were derived from the CPE parameters calculated by using the following equation [27].

$$C_{dl} = (Y_o . R_t^{1-n})^{1/n} \quad (6)$$

It is clear from Table 1 that R_t values increased with increase in the inhibitor concentration. The increase in R_t values is attributed to the formation of the protective film of the inhibitor on metal/solution interface. The increase in the value of 'n' of the inhibited samples in comparison to the uninhibited sample is due to decrease of the surface heterogeneity. Decrease in the surface heterogeneity is probably due to the adsorption of the inhibitors on the most active site of adsorption [28]. The value of the double layer capacitance (C_{dl}) decreased with increase in the cefadroxil concentration. The double layer capacitance (C_{dl}) is related to the thickness of the protective layer (d) by following equation [29].

$$C_{dl} = \frac{\varepsilon \varepsilon_o}{d} \quad (7)$$

where, ε is the dielectric constant of the protective layer and ε_o is the permittivity of the free space. Equation (7) suggests that C_{dl} is inversely proportional to the thickness of the protective layer (d). So the decrease in the double layer capacitance by increasing the inhibitor concentration shows increase in the thickness of protective layer.

It is clear from Table 1 that the cefadroxil inhibited the corrosion of mild steel in 1M HCl solution at every concentration used in the study. The inhibition efficiency (μ_{Rt} %) values are listed in Table 1. These values suggest that the inhibition efficiency increases with increase in the inhibitor concentration.

3.2. Potentiodynamic polarization measurements

The potentiodynamic polarization measurements were carried out to study the kinetics of the cathodic and anodic reactions. Figure 5 shows the results of the effect of cefadroxil inhibitor on the cathodic as well as anodic polarization curves of mild steel in 1M HCl respectively. It is evident from the figure that both reactions were suppressed with the addition of the cefadroxil inhibitor. This suggests that cefadroxil reduced the anodic dissolution reactions as well as retarded the hydrogen evolution reactions on the cathodic sites.

Electrochemical corrosion kinetic parameters namely corrosion potential (E_{corr}), corrosion current density (I_{corr}) anodic and cathodic Tafel slopes (b_a and b_c) obtained from the extrapolation of the polarization curves are listed in Table 2.

It is evident from Table 2 that the value of b_c changed with increase in inhibitor concentration and indicates the influence of the inhibitor on the kinetics of the hydrogen evolution. The shift in the anodic Tafel slope, b_a is due to the chloride ion/or inhibitor molecules adsorbed on the metal surface. The corrosion current density (I_{corr}) decreased by the increase in the adsorption of the inhibitor with increasing inhibitor concentration. According to Ferreira et.al [30] and Li et. al. [31], if the displacement in corrosion potential is more than 85 mV with respect to the corrosion potential of the

blank solution, the inhibitor can be consider as a cathodic or anodic type. In present study, maximum displacement was 14 mV with respect to the corrosion potential of the uninhibited sample which indicates that the studied inhibitor is a mixed type of inhibitor. The results obtained from the Tafel polarization showed good agreement with the results obtained from the EIS studies.

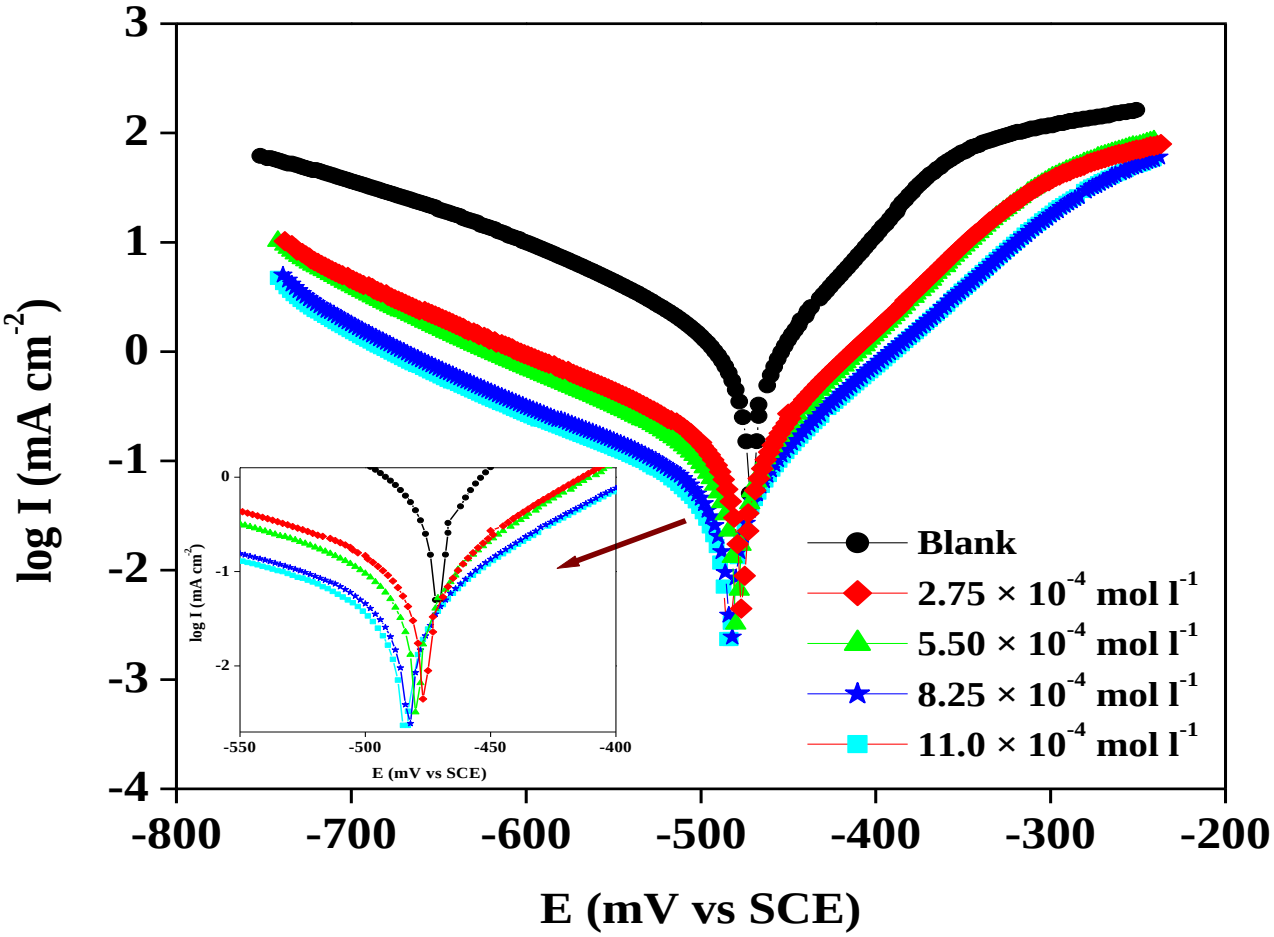

Figure 5. Tafel polarisation curves for corrosion of mild steel in 1M HCl in the absence and presence of different concentrations of Cefadroxil

3.3. Linear polarization resistance

Polarization resistance (R_p) values were determined from the slope of the potential current lines [27]:

$$R_p = A\frac{dE}{dI} \quad (8)$$

where A is the surface area of the electrode, dE is change in potential and dI is change in current. The inhibition efficiency and polarization resistance parameters are listed in Table 2. It is evident from the Table 2 that inhibition efficiency increases with increase in the polarization resistance and polarization resistance value increases with increase in the inhibitor concentration. The results

obtained from Tafel polarization and EIS showed good agreement with the results obtained from the linear polarization resistance.

Table 2. Potentiodynamic polarization parameters for the corrosion of mild steel in 1M HCl in absence and presence of different concentration of cefadroxil.

Inhibitor Concentration (10^{-4} ×Mol $^{-1}$)	**Tafel Polarization**					**Linear Polarization**	
	$-E_{corr}$ (mV vs SCE)	**b_a (mV/dec)**	**b_c (mV/dec)**	**I_{corr} (μA cm^2)**	**η_p (%)**	**R_p (Ω cm^2)**	**η_{Rp} (%)**
Blank	470	65.5	107.1	1540.0	-	14.0	-
2.75	476	73.5	154.4	180.0	88.3	102.1	86.3
5.50	480	69.6	143.0	104.0	93.2	153.5	90.9
8.25	483	76.2	166.1	65.6	95.7	239.3	94.2
11.0	484	73.5	161.8	54.6	96.5	292.5	95.2

3.4. Weight loss measurement

3.4.1. Effect of inhibitor concentration

The values of weight loss, inhibition efficiency (η_{WL} %), corrosion rate (CR) and surface coverage (θ) obtained from weight loss measurements at different concentrations of cefadroxil in 1M HCl at 308 K are summarized in Table 3.

Table 3. Corrosion parameters for mild steel in aqueous solution of 1N HCl in absence and presence of different concentrations of inhibitor from weight loss measurements at 308K for 3h.

Inhibitor concentration (10^{-4} × mol l^{-1})	**Weight loss (mg cm^{-2})**	**η_{WL} (%)**	**C_R (mm/y)**	**θ**
Blank	12.07	-	44.85	-
1.37	4.39	63.6	16.28	0.64
2.75	2.06	83.0	7.62	0.83
5.50	0.92	92.4	3.39	0.92
8.25	0.63	94.8	2.33	0.95
11.0	0.60	95.1	2.20	0.95
13.75	0.60	95.1	2.20	0.95

The variation of inhibition efficiency with increase in inhibitor concentrations is shown in Figure 6a. It was observed that Cefadroxil inhibits the corrosion of mild steel in HCl solution, at all the concentrations used in study. Maximum inhibition efficiency was exhibited at 11.0×10^{-4} mol l^{-1} cefadroxil inhibitor. It is evident from the Table 3 that the corrosion rate is decreased from 44.85 mm/y to 2.20 mm/y on the addition of 11.0×10^{-4} mol l^{-1} cefadroxil.

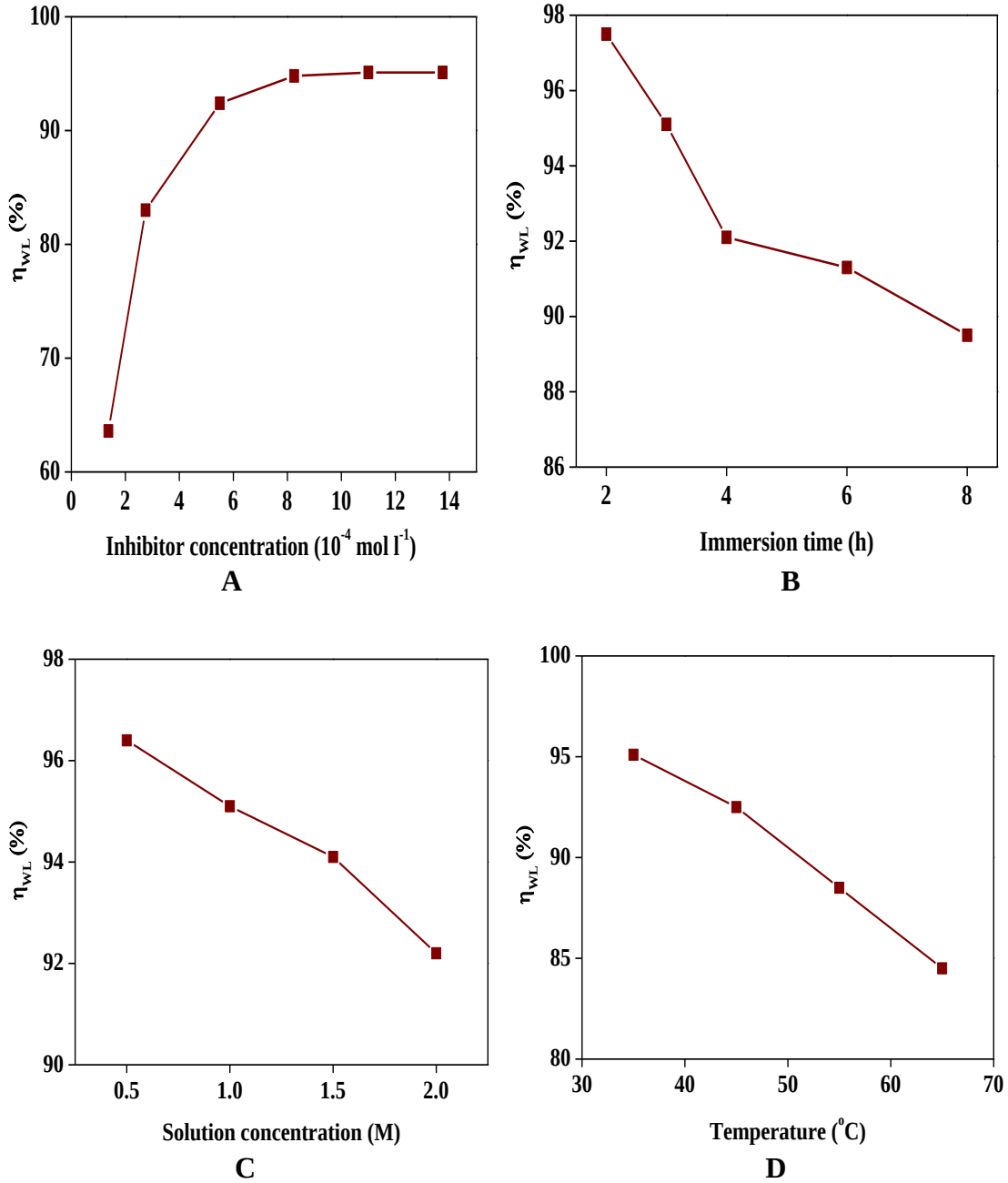

Figure 6. Variation of inhibition efficiency in 1M HCl on mild steel of surface area 20 cm^2 with (A) different concentrations of inhibitor; (B) different immersion time; (C) different acid concentration and (D) different temperature range; by using weight loss data.

3.4.2. Effect of immersion time

The effect of immersion time was investigated by using optimum concentration (11.0×10^{-4} mol l^{-1}) of cefadroxil for 2 to 8 hrs. The effect of immersion time on the inhibition efficiency is shown in Figure 6b. It is found that the inhibition efficiency decreases from 97.5% to 89.5% with increase in immersion time from 2 to 8 hrs.

3.4.3. Effect of acid concentration

The variation of inhibition efficiency with increase in acid concentration from 0.5 to 2.0 M with optimum concentration of inhibitor is shown in figure 6c. It is clear that change in acid concentration from 0.5M to 2.0M causes decrease in inhibition efficiency from 96.4% to 92.2%. This insignificant change in the inhibition suggests that the compound is effective corrosion inhibitor in acid solution over this concentration range.

3.4.4. Effect of temperature

Effect of solution temperature was studied at optimum concentration (11.0×10^{-4} mol l^{-1}) of inhibitor using the temperature range 308 - 338K. The influence of solution temperature on inhibition efficiency is shown in figure 6d. It is observed that inhibition efficiency decreased from 95.07% to 84.5% with increase in temperature from 308 - 338K. The decrease in inhibition efficiency with temperature may be attributed to desorption of the inhibitor molecule from metal surface at higher temperature [32].

3.5. Adsorption isotherm

Adsorption of inhibitor depends mainly on the charge and the nature of the metal surface, electronic characteristics of metal surface, temperature, adsorption of solvent, ionic species and on the electrochemical potential at solution interface. The adsorption isotherm study describes the adsorptive behavior of organic inhibitors in order to know the adsorption mechanism.

Table 4. Calculated parameters for Langmuir adsorption isotherm for mild steel in 1 M HCl in absence and presence of Cefadroxil at 308K.

Temperature (K)	**K_{ads} (mol^{-1})**	**Slope**	**R^2**	**$-\Delta G_{ads}$ (kJ mol^{-1})**
308	1.73×10^{-4}	0.99936	0.99962	35.27

The most frequently used adsorption isotherms are Langmuir, Temkin, Frumkin and Freundlich isotherms. In order to obtain the adsorption isotherm, the degrees of surface coverage (θ)

were calculated for various concentrations of the inhibitor from the weight loss data. Langmuir adsorption isotherm was tested to fit with the experimental data. Langmuir adsorption isotherm is represented by following equation:

$$\frac{C_{inh}}{\theta} = \frac{1}{K_{ads}} + C_{inh} \quad (9)$$

where K_{ads} is the adsorption equilibrium constant, θ is the degree of surface coverage and C_{inh} is molar concentration of inhibitor used in the corrosive solution. A straight line was obtained by plotting C_{inh} vs C_{inh} / θ for the inhibitor used in study with R^2 almost unity (0.99962) (Figure 7). This suggests that, the Langmuir adsorption isotherm provides the best description of the adsorption behavior. The degree of surface coverage (θ) for different inhibitor concentrations of cefadroxil was evaluated from weight loss data and listed in the Table 3. The slope of the isotherm graph reported in Table 4 is less than unity and this suggests the multilayer adsorption of the inhibitor molecule.

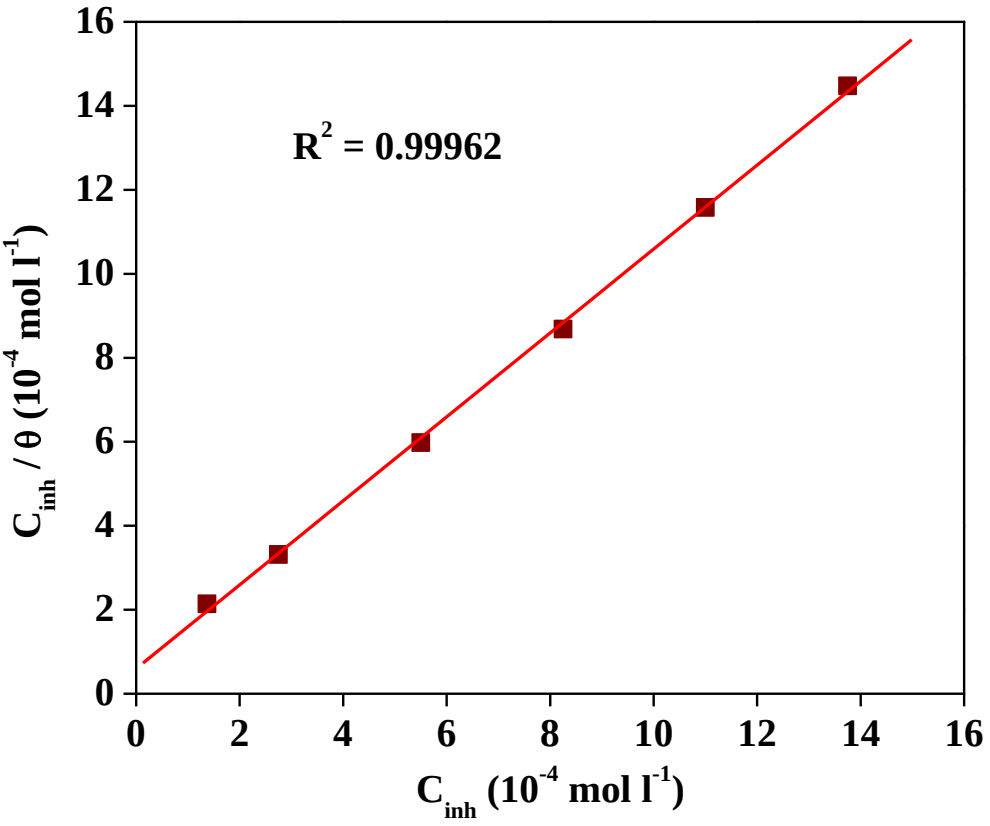

Figure 7. Langmuir's adsorption isotherm plots for the adsorption of cefadroxil 1M HCl on the surface of mild steel.

3.6. Kinetic and thermodynamic consideration

It has been reported by several authors [33, 34] that in acid solution, the logarithm of the corrosion rate is a linear function with 1 / T (Arrhenius equation):

$$\log(C_R) = \frac{-E_a}{2.303\ RT} + \log\lambda \qquad (10)$$

where, E_a is the apparent effective activation energy, R molar gas constant and λ the Arrhenius pre exponential factor.

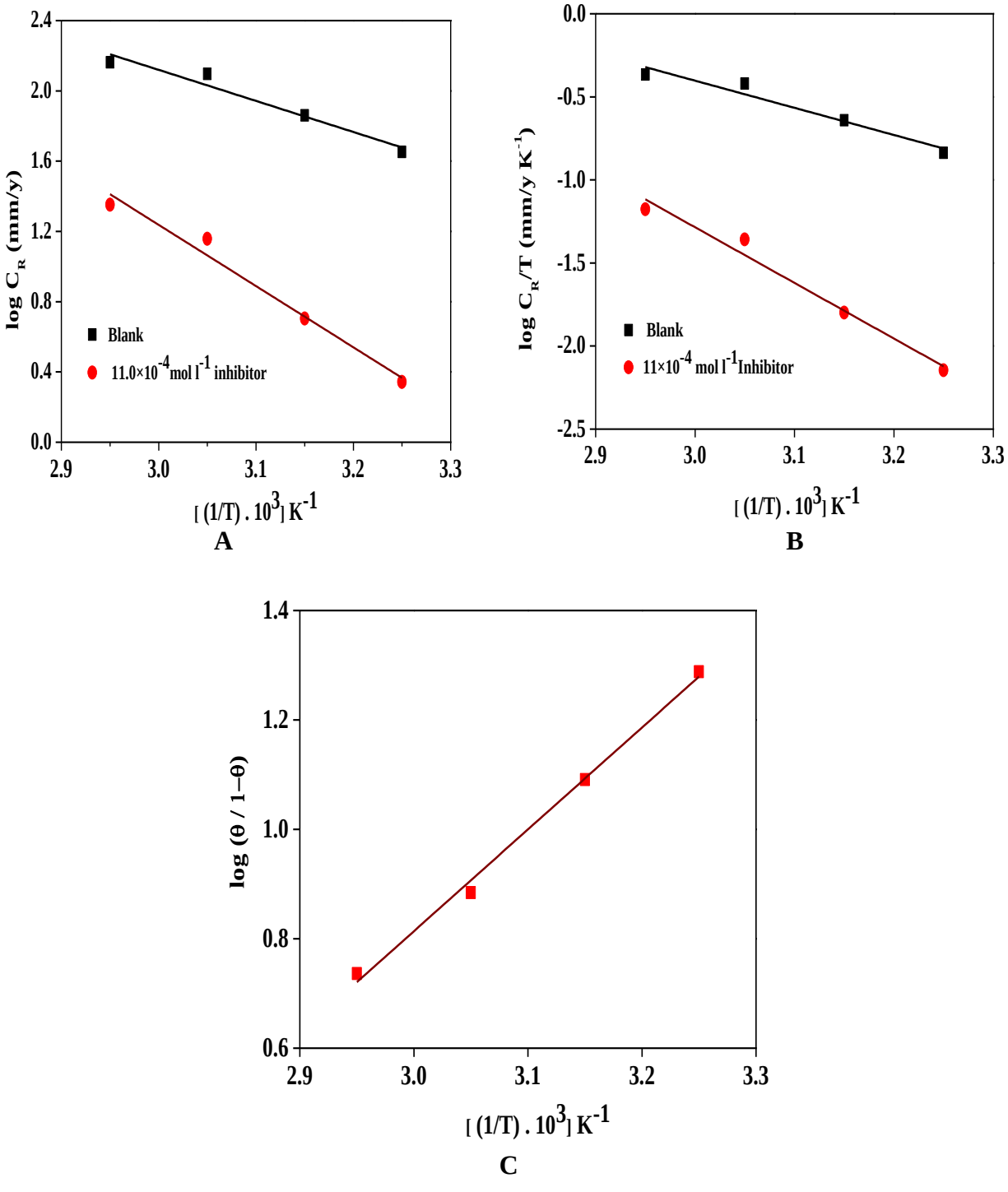

Figure 8. Adsorption isotherm plots in absence and presence of cefadroxil inhibitor in 1M HCl solution (A) *log* (C_r) versus *1/T* (B) log (C_r/T) versus *1/T* (C) *(θ/1-θ)* versus *1/T*

A plot of log of corrosion rate obtained by weight loss measurement versus 1/T gave straight line with regression coefficient close to unity, as shown in Figure 8a. The values of apparent activation energy (E_a) obtained from the slope ($-E_a/2.303R$) of the lines and the pre exponential factor (λ) obtained from the intercept (log λ) are given in Table 5. It is clear from the Table 5 that the apparent activation energy increased on addition of cefadroxil in comparison to the uninhibited solution. The increase in the apparent activation energy could be interpreted as physical adsorption.

Table 5. Thermodynamic parameters for mild steel in 1 M HCl in absence and presence of Cefadroxil

Inhibitor Conc. (10^{-4} × mol l^{-1})	**E_a (kJmol^{-1})**	**λ (mg cm^{-2})**	**ΔH^* (kJmol^{-1})**	**ΔS^* (Jmol^{-1}K^{-1})**	**ΔQ_{ads} (kJmol^{-1})**
Blank	33.85	2.66×10^{7}	31.28	-111.27	-
11.0	66.70	4.89×10^{11}	64.13	-29.61	-35.64

The increase in the activation energy can be attributed to an appreciable decrease in the adsorption of the inhibitor on mild steel surface with increase in the temperature. This leads to the increase in corrosion rate due to the greater area of metal that is exposed towards the corrosive environment [35]. The value of λ is also higher for inhibited solution than for the uninhibited solution. It is clear from the eq. (10) that corrosion rate is usually influenced by both E_a and λ. Generally, lower pre exponential factor (λ) and higher activation energy (E_a) leads to the lower corrosion rate. However, the effect of E_a on mild steel corrosion is larger than that of the λ. It is clear from the studies that decrease in the corrosion rate by increase in the inhibitor concentration suggests that the E_a is the deciding factor.

The dependence of corrosion rate on temperature can also be expressed using the transition state equation. An alternative formula for the Arrhenius equation is the transition state equation [36]:

$$C_R = \frac{RT}{NH} exp\left(\frac{\Delta S^*}{R}\right) exp\left(-\frac{\Delta H^*}{RT}\right) \quad (11)$$

where, h is Plank's constant, N the Avogadro's number, $\Delta S^*$the apparent entropy of activation and $\Delta H^*$the enthalpy of activation. A plot of *log (C_R/T)* versus *1/T* is shown in Figure 8(b). Straight lines were obtained with slope $(-\Delta H^*/2.303R)$ and intercept of $[log(R/Nh) + (\Delta S^*/2.303R)]$, from which ΔH^* and ΔS^*were calculated and listed in Table 5. It is clear from the Table 5 that the entropy of activation increased in the presence of inhibitor in comparison to the uninhibited sample. The increase in the activation entropy in presence of inhibitor indicates the increase in the disorderliness on going from reactant to activated complex. It is evident from the table that the value of ΔH^* increased in the presence of inhibitor than in the uninhibited solution indicating the higher inhibitive efficiency. This may be attributed to the presence of an energy barrier for the reaction, hence, the process of adsorption of inhibitor leads to rise in enthalpy of the corrosion process.

The heat of adsorption (ΔQ_{ads}) was obtained from the surface coverage and temperature by using following equation:

$$log\left(\frac{\theta}{1-\theta}\right) = logA + logC_{inh} - \left(\frac{\Delta Q_{ads}}{2.303RT}\right) \quad (12)$$

A plot of $\log(\theta/1-\theta)$ vs $1/T$ is given in Figure 8c. The value of heat of adsorption was determined from the slope $(-\Delta Q_{ads}/2.303R)$ of the graph. The value of heat of adsorption is given in Table 5. It is evident from the Table 5 that ΔQ_{ads} has negative value which indicates that inhibitor adsorption decreases with increase in the temperature hence decrease in inhibitor efficiency [37]. The negative value of ΔQ_{ads} also suggested that the adsorption of inhibitor is an exothermic process [38].

Free energy of adsorption (ΔG_{ads}) was calculated using the following equations [39]:

$$K_{ads} = \frac{1}{55.5}\ exp\left[\frac{-\Delta G^{o}_{ads}}{RT}\right] \quad (13)$$

This equation can also be express in the form as follows:

$$\Delta G_{ads} = -2.303\ RT \log(55.5K_{ads}) \quad (14)$$

where ΔG_{ads} is Gibbs free energy of adsorption, T is the temperature in Kelvin and K_{ads} is the equilibrium constant for the adsorption process and 55.5 is the molar concentration of water in solution. K_{ads} value was calculated from the intercept of the Figure 7 and presented in table 4. ΔG_{ads} values calculated using eq.14 is presented in Table 4. The negative value of Gibbs free energy ensures the spontaneity of adsorption process and stability of the adsorbed layer on the surface of mild steel.

3.7. Surface characterization

To establish whether inhibition is due to the formation of adsorbed film on the metal surface, atomic force micrographs were taken. The AFM micrographs are shown in Figure 9(a-c). The average roughness of the polished mild steel (Figure 9a) and mild steel in 1.0M HCl solution without inhibitor (figure 9b) was calculated as 48 and 471 nm, respectively. The mild steel surface in the free acid solution is getting cracked due to the acid attack on the surface (figure 9b). However, in presence of 11×10^{-4} mol l^{-1}cefadroxil, the average roughness was reduced to 139 nm.

3.8. Mechanism of inhibition

Corrosion inhibition of mild steel in 1M HCl by cefadroxil can be explained on the basis of molecular adsorption of inhibitor on to the metal surface. It is generally considered that the first step in the corrosion inhibition of a metal is the adsorption of the inhibitor molecules at metal/solution interface [40]. Organic compounds are adsorbed on the metal surface by (i) electrostatic interaction between the charged molecules and charged metal; (ii) interaction of π-electrons with the metal; (iii)

interaction of unshared pair of electrons in the molecule with the metal; and (iv) the combination of the all the effects [41,42].

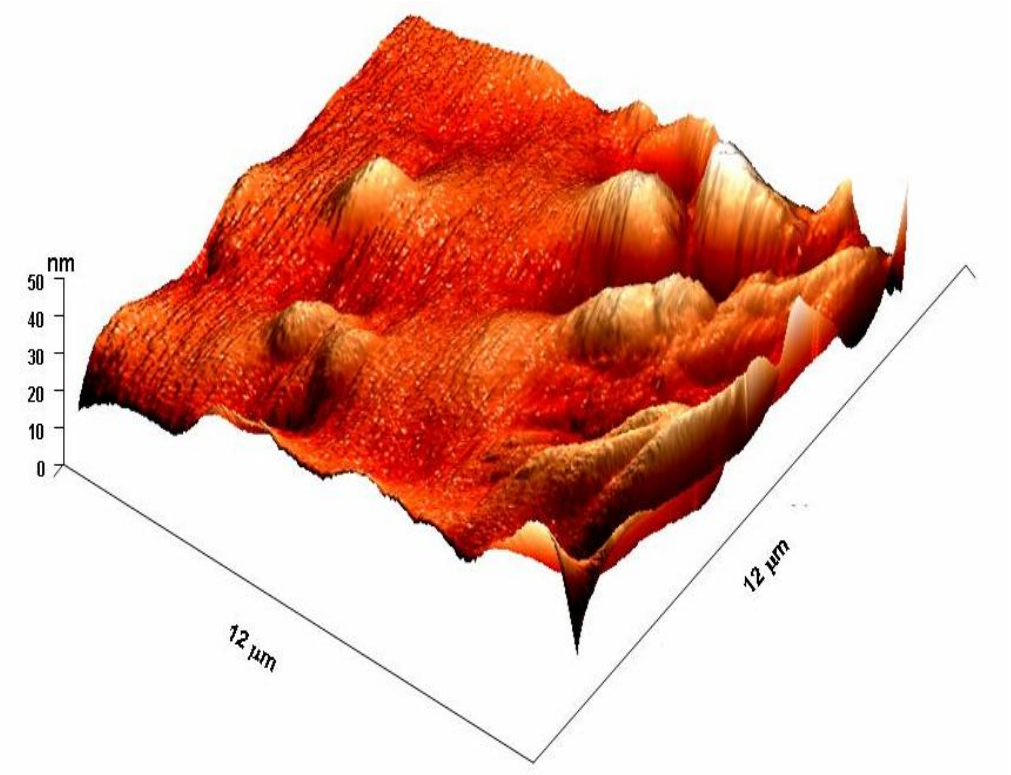

A

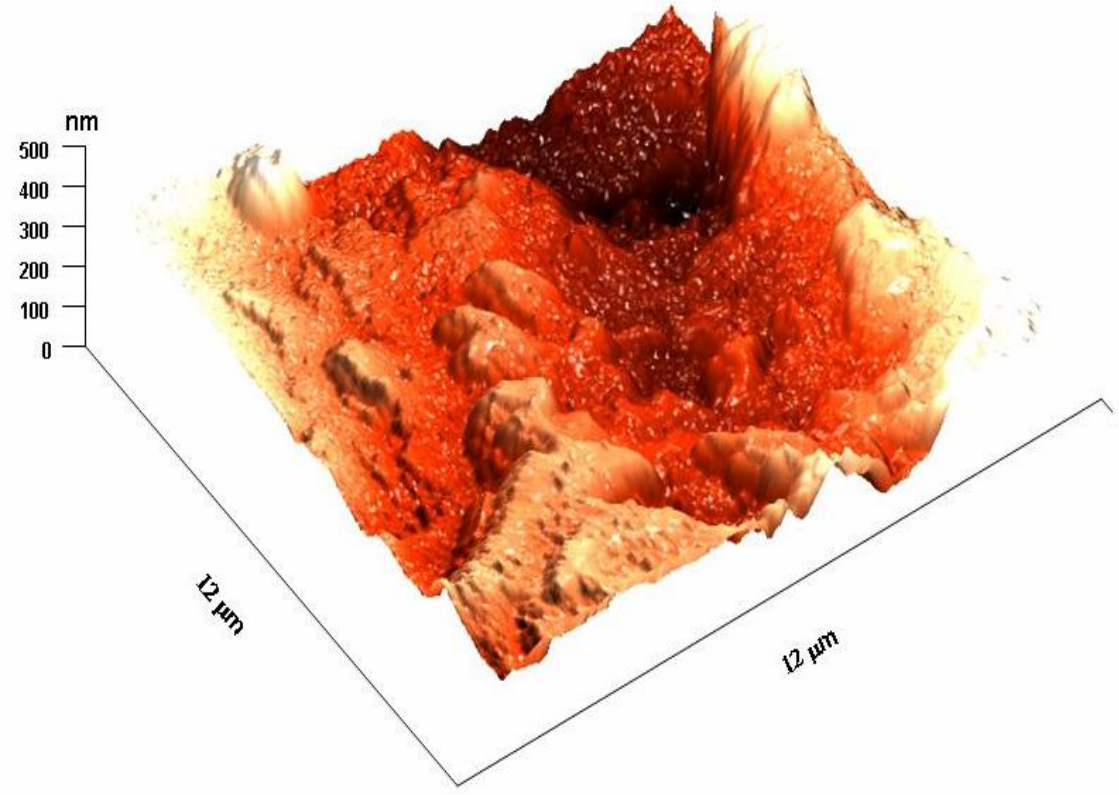

B

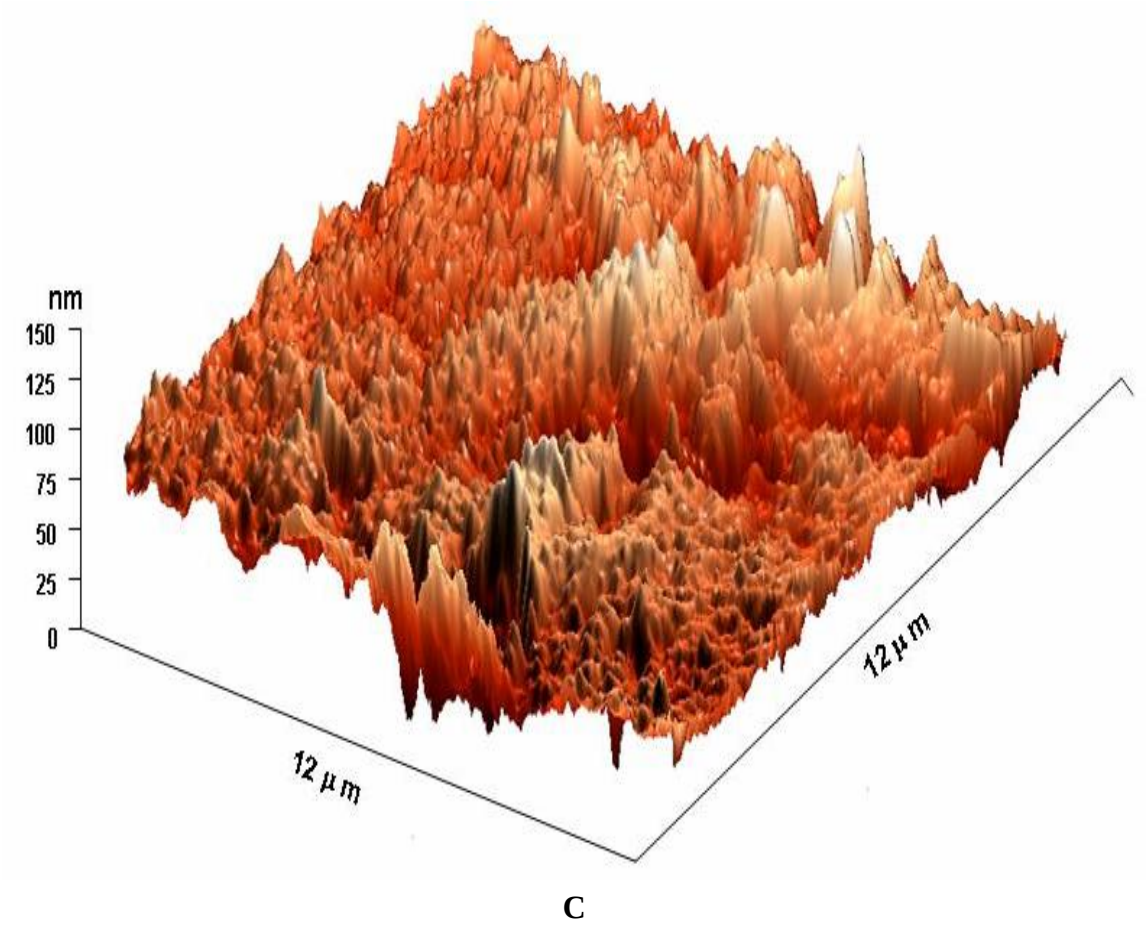

Figure 9. Atomic force micrograph of (A) Polished mild steel surface (B) mild steel exposed in 1M HCl (C) mild steel exposed in (1M HCl +11.0 $\times 10^{-4}$ mol l^{-1}).

The inhibition efficiency of the inhibitors also depends on many factors such as the adsorption centers, mode of interaction with metal surface, charge density, molecular size, and the formation of the metallic complexes [43-45]. Physical adsorption of the inhibitor molecule requires both electrically charged surface of the mild steel and charged inhibitor species in the corrosive solution. The inhibitor molecule is protonated in the acid medium. Thus they become cation, existing in equilibrium with the corresponding molecular form. It is well known that the steel surface bears positive charge in acid solution [46]. The protonated inhibitor molecule could be attached to the mild steel surface by electrostatic interaction between Cl^- and protonated cefadroxil [47]. The decrease in the inhibition efficiency obtained with rise in the temperature supports the electrostatic interaction.

4. CONCLUSION

All the measurements showed that the cefadroxil has excellent inhibition properties against the mild steel corrosion in hydrochloric acid solution. EIS measurements also indicates that the inhibitor performance increase due to the adsorption of molecule on the metal surface. Potentiodynamic

polarization measurements showed that the inhibitor acts as mixed type of inhibitor. The inhibitor showed maximum inhibition efficiency (approx 96%) at 11.0×10^{-4} mol l^{-1} concentration of the studied inhibitor. The inhibition efficiencies determined by EIS, potentiodynamic polarization and weight loss studies are in good agreement. The inhibitor follows the Langmuir adsorption isotherm in the process of adsorption. Thermodynamic calculations show that the adsorption process is spontaneous, exothermic and follow the physical adsorption mechanism on the metallic surface. Atomic force microscopic studies showed that there is decrease in the surface roughness of inhibited surface in comparison with the uninhibited surface in hydrochloric acid solution.

ACKNOWLEDGEMENT
SKS acknowledges the North West University for a Postdoctoral Fellowship.

References

1. S.A. Umoren, I.B. Obot and E.E. Ebenso, *E-Journal of Chemistry*, 5 (2008) 355.
2. A. K. Mishra and R. Balasubramaniam**,** *Mater. Chem. Phys.* 103 (2007) 385.
3. F. Bentiss, M. Lebrini, M. Traisnel, M. Lagrenee, *J. Appl. Electrochem.* 39 (2009) 1399.
4. M.A. Quraishi, S.K. Shukla, *Mater. Chem. Phys.* 113 (2009) 685-689.
5. I.B. Obot, N.O. Obi-Egbedi, S.A. Umoren, E.E. Ebenso, *Int. J. Electrochem. Sci.,* 5 (2010) 994.
6. M.A. Quraishi, I. Ahamad, A.K. Singh, S. K. Shukla, B. Lal, V. Singh, *Mater. Chem. Phys.* 112 (2008) 1035.
7. S. K. Shukla, M.A. Quraishi, *J. Appl. Electrochem.* 39 (2009) 1517.
8. S.K. Shukla, M.A. Quraishi, R. Prakash, *Corros. Sci.* 50 (2008) 2867.
9. S.K. Shukla, M.A. Quraishi, *Mater. Chem. Phys.* 120 (2010) 142.
10. S.K.Shukla, M.A. Quraishi, *Corros. Sci*, 52(2010)314.
11. M. S. Morad, *Corros. Sci.* 50 (2008) 436.
12. S.K.Shukla, M.A. Quraishi, *Corros. Sci,* 51(2009)1007.
13. S.K. Shukla, A.K. Singh, I. Ahamad, M. A. Quraishi, *Mater. Lett.* 63(2009)819.
14. M. Abdallah, *Corros. Sci.* 46 (2004) 1981.
15. A.A. Harmas, M.S. Morad, M.H. Wahdan, *J. Appl. Electrochem.* 34 (2004) 95.
16. S.S. Abdel Rehim, H.H. Hasan, M.A. Amin, *Appl. Surf. Sci.* 187 (2002) 279.
17. C. Deslouis, B. Tribollet, G. Mengoli, M.M. Muisani, *J. Appl. Electrochem.* 18(1988) 374.
18. S. K. Shukla, M.A. Quraishi, *Corros. Sci*. 51 (2009) 1990.
19. K. Juttner, *Electrochimica Acta,* 35 (1990) 1501.
20. W.R. Fawcett, Z. Kovacova, A. Motheo, C. Foss, *J. Electroanal. Chem.* 326 (1992) 91.
21. S.O. Niass, M.E. Touham, N. Hajjaji, A. Srhiri, H. Takenouti, *J. Appl. Electrochem.* 31 (2001) 85.
22. A.K. Singh, S.K. Shukla, M. Singh, M.A. Quraishi, *Mater. Chem. Phys*. (2011) doi: 10.1016/jmatchemphys.2011.03.054.
23. F. Mansfeld, *Corrosion* 36 (1981)301.
24. J.R. Mcdonald, *J. Eectroanal. Chem.* 223 (1987)25.
25. J. Pang, A. Briceno, S. Chander, *J. Electrochem. Soc.* 137 (1990) 3447.
26. U. Rammelt, G. Reinhard, *Corros. Sci.* 27 (1987)373.
27. A.K. Singh, M.A. Quraishi, *J. Appl. Electrochem.* 41 (2011) 7.
28. M. Lebrini, M. Lagrenee, H. Vezin, M. Traisnel, F. Bentiss, *Corros. Sci.* 49 (2007) 2254.
29. H.H. Hassan, *Electrochim, Acta,* 51 (2006) 5966.
30. E.S. Ferreira, C. Giancomelli, F.C. Giacomelli, A. Spinelli, *Mater. Chem. Phys.* 83 (2004) 129.

31. W.H. Li, Q. He, C.L. Pei, B.R. Hou, *J. Appl. Electrochem*. 38 (2008) 289.
32. M. Schorr, J. Yahalom, *Corros. Sci.* 12 (1972) 867.
33. C.B. Breslin, W.M. Carrol, *Corros. Sci*. 34 (1993) 327.
34. M.G.A. Khedr, M.S. Lashien, *Corros. Sci.* 33 (1992) 137.
35. T. Szauer, A. Brandt, *Electrochim Acta* 26 (1981) 1253.
36. S.S.A. Rehim, H.H. Hassan, A.A. Mohammed, *Mat. Chem. Phys.*, 70 (2001) 64.
37. H.M. Bhajiwala, R.T. Vashi, *Bull. Electrochem.* 17 (2001) 441.
38. X.H. Li, G.N. Mu, *Appl. Surf. Sci.* 252 (2005) 1254.
39. M. Schorr, J. Yahalom, *Corros. Sci*, 12 (1972) 867.
40. M. Sahin, S. Bilgic, H. Yilmaz, *Appl. Surf. Sci*.195 (2002) 1.
41. H. Shorky, M. Yuasa, I. Sekine, R.M. Issa, H.Y. El-Baradie, G.K. Gomma, *Corros. Sci.* 40 (1998) 2173.
42. D.P. Schweinsberg, G.A. George, A.K. Nanayakkara, D.A. Steiner, *Corros. Sci.* 28 (1988) 33.
43. A. Fouda, M. Moussa, F.I. Taha, A.I. ElNeanaa, *Corros. Sci.* 26 (1986) 719.
44. E.A. Noor *Corros. Sci.* 47 (2005) 33.
45. F. Bentiss, C. Jama, B. Mernari, H. El-Attari, L. El-Kadi, M. Lebrini, M. Traisnel, M. Lagrenee, *Corros. Sci.* 51 (2009) 1628.
46. G.N. Mu, T.P. Zhao, M. Liu, T. Gu, *Corrosion*, 52 (1996) 853.
47. G. Banerjee, S.N. Malhotra, *Corrosion,* 48 (1992) 10.